



HAL
open science

Magnetism without magnetic impurities in oxides ZrO₂ and TiO₂

Frantisek Maca, Josef Kudrnovsky, Vaclav Drchal, Georges Bouzerar

► **To cite this version:**

Frantisek Maca, Josef Kudrnovsky, Vaclav Drchal, Georges Bouzerar. Magnetism without magnetic impurities in oxides ZrO₂ and TiO₂. Philosophical Magazine, 2008, 88 (18-20), pp.2755-2764. 10.1080/14786430802342584 . hal-00513943

HAL Id: hal-00513943

<https://hal.science/hal-00513943>

Submitted on 1 Sep 2010

HAL is a multi-disciplinary open access archive for the deposit and dissemination of scientific research documents, whether they are published or not. The documents may come from teaching and research institutions in France or abroad, or from public or private research centers.

L'archive ouverte pluridisciplinaire **HAL**, est destinée au dépôt et à la diffusion de documents scientifiques de niveau recherche, publiés ou non, émanant des établissements d'enseignement et de recherche français ou étrangers, des laboratoires publics ou privés.



Magnetism without magnetic impurities in oxides ZrO_2 and TiO_2

Journal:	<i>Philosophical Magazine & Philosophical Magazine Letters</i>
Manuscript ID:	TPHM-08-May-0174
Journal Selection:	Philosophical Magazine
Date Submitted by the Author:	16-May-2008
Complete List of Authors:	Maca, Frantisek; Institute of Physics AS CR, Theoretical Kudrnovsky, Josef; Institute of Physics AS CR, Condensed Matter Theory Drchal, Vaclav; Institute of Physics AS CR, Condensed Matter Theory Bouzerar, Georges; Institut Laue Langevin; Institut Neel CNRS
Keywords:	density-functional methods, magnetism, oxides
Keywords (user supplied):	impurity



RESEARCH ARTICLE

Magnetism without magnetic impurities in oxides ZrO_2 and TiO_2

František Máca¹, Josef Kudrnovský¹, Václav Drchal¹, and Georges Bouzerar^{2,3}

¹Institute of Physics ASCR, Na Slovance 2, CZ-182 21 Prague 8, Czech Republic

²Institut Néel, 25 avenue des Martyrs, CNRS, B.P. 166, 38042 Grenoble Cedex 09, France

³Institut Laue Langevin, B.P. 156, 38042 Grenoble Cedex 09, France

(Received 00 Month 200x; final version received 00 Month 200x)

We apply the density functional technique to investigate the magnetism induced in transition metal dioxides ZrO_2 and TiO_2 by substitution of the cation by a vacancy or an impurity from the groups 1A or 2A of the periodic table, where the impurity is either K or Ca. It is demonstrated that the vacancy and the K-impurity leads to a robust induced magnetic moment on the surrounding O-atoms for both the cubic ZrO_2 and rutile TiO_2 host crystals. The native O-vacancy does not induce a magnetic moment in the host dioxide crystal.

Keywords: magnetism; impurity; oxides; density functional calculations

1. Introduction

We are all used when we refer to magnetic materials to have in mind systems which at least contain the essential brick, the magnetic impurities such as Fe, Ni or Mn. However, it has been reported several times that magnetism can also be observed in materials which do not contain such magnetic impurities. Ferromagnetism in this new class of materials is referred to as "d⁰" or intrinsic ferromagnetism. Experimentally, it has been shown that thin films of HfO_2 and ZrO_2 [1, 2] exhibit very high Curie temperature (above room temperature). Unexpected ferromagnetism has been also reported in irradiated graphite [3, 4] and even in La-doped hexaborides such as CaB_6 [5]. Theoretically, ferromagnetism was predicted in systems, where the Fermi level lies in a flat band [6, 7]. Recently it has been shown that $CaAs$ is a good candidate for flat band ferromagnetism [8].

However, the intrinsic ferromagnetism is often a subject of controversy. For example, it has been argued that the ferromagnetism in CaB_6 is due to the presence of magnetic impurities such as Fe [9]. In addition, intrinsic ferromagnetism often appears difficult to be stabilized and controlled as it strongly depends on the sample history: materials grown under similar conditions may lead to non-magnetic samples. Until now, there is no clear understanding of the underlying mechanism which is at the origin of the observed magnetism. From a theoretical point of view, it has been shown that point defects as cation vacancies may be at the origin of the magnetism in these materials [10–13]. The vacancy induces in these materials local magnetic moments on the neighboring oxygen atoms which then interact with relatively extended exchange couplings. The oxygen vacancies were originally also suggested as a source of the magnetism in HfO_2 [14], but the density functional calculations [12] found no evidence for the formation of magnetic moments around such defects.

The long-range ferromagnetic order is possible only if the exchange couplings are extended enough (beyond the percolation threshold). Osorio-Guillen *et al.* [13] have shown that in CaO oxide the ferromagnetism induced by cation vacancies is possible only if the density of vacancies is sufficiently large (above 5%). They found that the formation energy of a vacancy is relatively high, which implies that the cation vacancy induced ferromagnetism is unlikely.

A progress has been done recently in the understanding of the "d⁰" ferromagnetism [15] in the framework of a minimal model which includes the effects of disorder and electron-electron correlation effects on equal footing. The effect of the cation vacancy or non-magnetic impurity on neighboring oxygen orbitals (the correlated disorder) is the relevant part of the theory. This study has predicted that very high Curie temperatures can be reached for realistic parameters. It was shown that the optimal situation for ferromagnetism depends mainly on two parameters (i) the position of the impurity band which should be on the edge to split from the valence band for the hole doped case, and (ii) the density of holes per defect should be of the order of three. In order to circumvent the

difficulties of controlling intrinsic defects such as vacancies, an alternative way which consists in the substitution of the four-valent cation A^{4+} in dioxides such as AO_2 ($A=Ti, Zr, Hf$) by a single-valent cation of the group 1A of the periodic table has been proposed. The substitution of the four-valent host A^{4+} by a single-valent impurity X^+ , where $X=K, Li, Na, \text{ or } Cs$, introduces three holes per impurity. However, we should emphasize that it is not granted that the system will become magnetic and that the impurity band will be located near the top of the valence band.

In this paper we shall address a question concerning the formation of magnetic moments in the host dioxides doped by non-magnetic impurities. To this end we perform an *ab initio* study of the effect of substitution of the cation by an element of the group 1A or 2A. We employ the supercell approach using the full-potential linearised augmented plane-wave method (FLAPW) [16]. The single impurity in the supercell with increasing size corresponds to decreasing impurity concentration. The approach allows electronic relaxations on the sites neighboring impurity which are essential for the formation of induced non-local magnetic moments in such systems as the A-vacancy in AO and AO_2 oxides [11–13]. We have also investigated the case of two nearest-neighbor impurities that have a common nearest neighbor oxygen site and the effect of group 2A impurities (such as Ca) which introduce only two holes per Ca-impurity when substituting the A-cation in AO_2 oxides.

2. Formalism

We consider a tetragonal supercell consisting of two conventional cells for the fluorite structure of ZrO_2 and four tetragonal units for the TiO_2 rutile structure. It is constructed by doubling the area of the basis in the xy plane, and in the case of TiO_2 also along the c axis. The supercell contains 8 molecular units of the host dioxide and its lattice parameter are $(\sqrt{2}a, \sqrt{2}a, a)$ for the fluorite structure and $(\sqrt{2}a, \sqrt{2}a, 2c)$ for the rutile structure. The substitutional impurity is introduced in the centre of the supercell XA_7O_{16} which corresponds to an effective impurity concentration of 12.5%. We neglect the change of the lattice constant due to impurity as well as local relaxations. We have used the experimental lattice constants $a=5.256 \text{ \AA}$ for fluorite ZrO_2 [17] and $a = b = 4.59 \text{ \AA}$, $c = 2.96 \text{ \AA}$ for the rutile TiO_2 [18]. We have also considered larger supercells corresponding to lower effective concentrations, namely, the $XA_{31}O_{64}$ supercell (concentration of 3.125%) with lattice parameters $(2a, 2a, 2a)$ for the fluorite and $(2a, 2a, 4c)$ for the rutile structures, respectively.

The spin-polarized electronic structure was obtained by the FLAPW method as implemented in the WIEN2k program package [16] with the Perdew-Wang exchange-correlation potential [19]. We employed a plane-wave cutoff energy $E_{cut} = 16 \text{ Ry}$ and 40 special points in the irreducible wedge of the Brillouin zone of the large supercell with 96 atoms and correspondingly higher number of points for smaller supercells.

The local magnetic moments are obtained by integrating over the muffin-tin spheres. Radii 2.35 a.u. and 1.7 a.u. for K/Zr and O in ZrO_2 , respectively and 2.0 a.u. and 1.6 a.u. for K/Ti and O in TiO_2 , respectively were used.

3. Results and discussions

Two kinds of impurities were considered, namely vacancies and K-dopants in both oxides. Test calculations were also done for Ca-dopants in TiO_2 , and for the nearest neighbor X–O–X complex in ZrO_2 ($X=$ vacancy, K-impurity).

The results are presented for ZrO_2 and for TiO_2 , respectively, using the FLAPW method for two effective impurity concentrations of 3.125% and 12.5% corresponding to 96- and 24-atom supercells.

We have found no induced magnetic moment in the host due to native O-vacancies either in ZrO_2 or in TiO_2 . Similar results were found by Das Pemmaraju and Sanvito [12] for O-vacancies in HfO_2 .

3.1. Impurities in ZrO_2

Both vacancy and K-impurity on Zr-cation sublattice give rise to a well defined robust magnetic moment induced on neighboring shells of O-atoms. Note that the value of this moment could vary with the impurity concentration. We first discuss the case of a vacancy. For a relatively low concentration of 3.125% the total induced moment in the supercell is $4 \mu_B$. We found that the induced moment decreases slightly to $3.86 \mu_B$ for a higher concentration of 12.5%. The relevant part of the induced magnetic moment is mainly located on the first shell of host O-atoms ($0.38/0.40 \mu_B$ for lower/higher concentration). The induced moments on the next oxygen shell ($0.03/0.05 \mu_B$) are an order of magnitude smaller. The moment on Zr-atoms neighboring the defect are negligible ($-0.01/-0.03 \mu_B$). Despite the smallness of induced moments on O-sites, the total moment is large because of the number of equivalent atoms in each shell neighboring the impurity is large (8 in the first shell, 24 in the second shell). Again, these results are similar to those of Ref. [12] for

vacancies in the monoclinic HfO_2 crystal. Of course, the magnitude of the induced moments could be quantitatively influenced by possible lattice relaxation as discussed in Ref. [12].

We now discuss the K-cation impurity. In this case we have also found an induced moment but slightly smaller than that of vacancy. Here, on the contrary, the system tends to a halfmetallic behavior for sufficiently high concentration of defects. The total induced moment slightly increases with the impurity concentration ($2.67/2.99 \mu_B$). As expected, the total induced moment is smaller roughly by one μ_B than that of vacancy. Indeed, K-impurity brings only three holes as compared to four holes in the case of a vacancy. Similarly to the case of vacancy, magnetic moments induced on more distant O-atoms ($0.03/0.05 \mu_B$) are an order of magnitude smaller than on O-atoms close to the impurity ($0.21/0.30 \mu_B$) but they are nevertheless important as they help to overcome the magnetic percolation threshold. The magnetic moments on other sites (impurity and neighboring Zr atoms) are again negligible. Because the induced moment around the cation impurities is rather extended, the corresponding percolation threshold is expected to be much smaller as compared to that of conventional local magnetic moments e.g. in GaAs:Mn or GaN:Mn alloys. This is a particularly interesting result for the substitutional K-cation impurity which can be more easily controlled experimentally than the intrinsic defects.

In the framework of the supercell approach we have also investigated the possibility of induced magnetic moments due to Ca-substitutional impurity in ZrO_2 . We have found no induced moment in this case. This result is in agreement with a general conclusion made in [15], namely that the optimal situation for magnetism in dioxides requires impurities which release three holes per defect into the valence/impurity band. Thus, we find a decreasing tendency to form an induced magnetic moment in ZrO_2 if Zr is substituted by vacancy, K, and Ca. This result can be understood qualitatively as a consequence of decreasing the charge difference between the host and impurity cation. Such a qualitative explanation could be supported by a simple Stoner-picture model. We present in Fig. 1 the total densities of

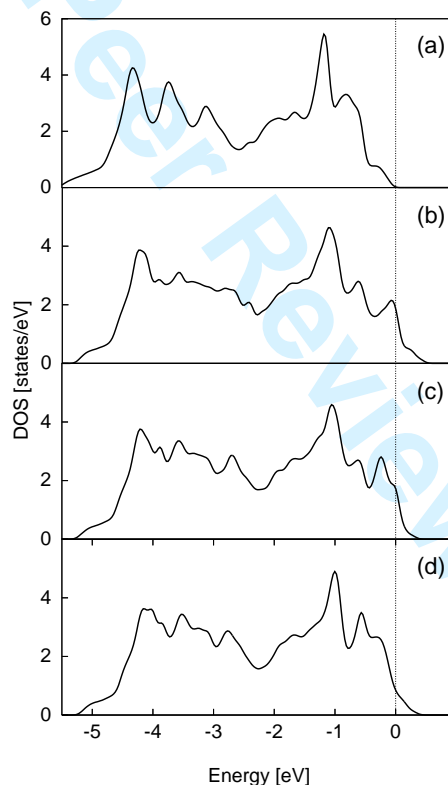


Figure 1. The total densities of states per formula unit for various impurities in the cubic nonmagnetic ZrO_2 : (a) ZrO_2 host; (b) vacancy in ZrO_2 ; (c) K in ZrO_2 ; and (d) Ca in ZrO_2 . Calculations were performed for the supercell $\text{XZr}_{15}\text{O}_{32}$ corresponding to the effective impurity concentration of 6.25%. The energy zero indicates the Fermi energy.

states (DOS) of the nonmagnetic phase calculated using the supercell approach in the limit corresponding to the effective impurity concentration of 6.25% ($\text{XZr}_{15}\text{O}_{32}$, X=vacancy, K, Ca). A strong reduction of the total density of states at the Fermi energy for Ca-impurity as compared to K-impurity and vacancy is clearly seen. This explains the decreasing tendency to form an induced magnetic moment.

Using the embedded cluster method[20] (ECM) based on the Green function approach as implemented recently in the framework of the tight-binding linear muffin-tin orbital

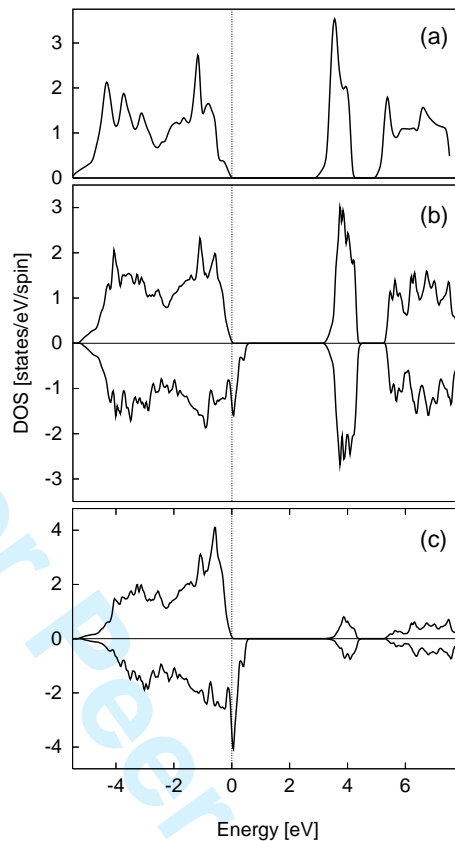


Figure 2. (a) The total density of states per formula unit for ZrO₂ host and (b) the spin resolved densities of states for KZr₇O₁₆ supercell. (c) The spin-resolved local densities of states per formula unit on the first O-shell surrounding the impurity for the cubic KZr₇O₁₆ supercell. The effective K-impurity concentration is 12.5%. The energy zero indicates the Fermi energy.

(TB-LMTO) method [21, 22] we have also investigated the case of two nearest-neighbor vacancies/K-impurities in the ZrO₂ host that have two equivalent nearest-neighbor oxygen sites. The ECM approach allows us to address the problem of moment formation for localized defects in the infinite host crystal. The total induced moment on O-sites inside the cluster is strongly enhanced when compared to the case of a single impurity: $7.1 \mu_B$ for two vacancies and $4.85 \mu_B$ for two K atoms. This should be compared with the values of $3.93 \mu_B$ and $2.62 \mu_B$ found for a single vacancy and K-impurity. The local moment on O atoms neighboring the impurity is strongly enhanced, namely $1.22 \mu_B$ and $0.77 \mu_B$ for the vacancy and K-impurity, respectively. The other induced moments are similar to those found for a single impurity case. One could conclude that the nearest-neighbor X-O-X cluster (X=vacancy or K) induces in ZrO₂ host a larger and more extended magnetic moment.

The spin resolved total DOS and local DOS on O-sites for substitutional K-impurity in ZrO₂ are shown in Fig. 2 for the KZr₇O₁₆ supercell (12.5% of impurities). The substitutional K-impurities in ZrO₂ polarize the host band giving rise to well split spin-subbands. The induced impurity peak close to the valence band edge is seen in the minority DOS while the majority DOS is influenced by impurities only negligibly (compare Fig. 2(a) and 2(b)). This effect is even more clearly seen in the O-local DOS shown in Fig. 2(c) from which it is found that the valence band is formed predominantly by the oxygen *p*-states. The above results are again in a qualitative agreement with those of Ref. [15]. Namely, the presence of an impurity band close to the top of the valence band is a precursor for the appearance of magnetism in dioxides. This is the case for both a vacancy and substitutional K-impurity (see Fig. 1(b),(c)). In contrast, for Ca substitution, the impurity band is shifted deeper into the valence band, which prevents the formation of a magnetic moment.

3.2. Impurities in TiO₂

We have also investigated the possibility for non-magnetic impurity induced magnetism in TiO₂. We used similar supercells, namely XTi₇O₁₆ and XTi₃₁O₆₄ as in the case of ZrO₂ (effective concentrations are 12.5% and 3.125%). The main results (see Table 1) are in qualitative agreement with those for the cubic ZrO₂ structure. Nevertheless, for higher

concentration of vacancies (12.5%) no magnetic state has been found in TiO_2 . For smaller concentrations both vacancy and substitutional K-impurity induce magnetic moments on the surrounding O-sites and the sizes of total induced moments are similar in ZrO_2 and TiO_2 . There are, however, some quantitative differences due to different lattices. In the rutile structure there are four equivalent nearest-neighbor O-sites and two other next nearest-neighbor O-sites with almost the same distance from the Ti-/impurity site. Lattice anisotropy leads to a different distribution of the induced moments.

Table 1. The total magnetic moment per cell (M_{cell}) and local magnetic moments on the impurity (m_X) and on the nearest neighbors host atoms adjoining it for two cubic supercells, $\text{XTi}_7\text{O}_{16}$ and $\text{XTi}_{31}\text{O}_{64}$, corresponding to effective impurity concentrations of 12.5% and 3.125%, respectively. Here m_{O_1} , m_{O_2} , and m_{Ti_1} denote atoms in corresponding nearest-neighbor shells of the host. The impurity atoms are X=vacancy, and K. All magnetic moments are given in units of μ_B .

impurity X	m_X	m_{O_1}	m_{O_2}	m_{Ti_1}	M_{cell}
vacancy (12.5%)	–	0.00	0.00	0.00	0.00
vacancy (3.125%)	–	0.44	0.28	–0.04	3.46
K (12.5%)	0.27	0.05	0.32	0.00	2.10
K (3.125%)	0.35	0.31	0.18	0.01	2.91

We have also checked the effect of local structure relaxations in the vicinity of impurity for the case of $\text{KTi}_7\text{O}_{16}$. The distance between the K-impurity and four nearest neighbor O1 oxygen sites increases from 1.95 \AA to 2.27 \AA and between two O2 oxygen sites from 1.98 \AA to 2.15 \AA . The existence of induced moment due to K-impurity is not influenced, the total induced moment changes from $2.10 \mu_B$ to $2.08 \mu_B$, the local moments on O1-sites change from $0.32 \mu_B$ to $0.26 \mu_B$ while the local moments on O2-sites remain unchanged ($0.05 \mu_B$).

The induced local moments are different for different impurity concentrations, e.g. on O2 sites is local magnetic moment $0.19 \mu_B$ for a concentration of 3.125% but becomes $-0.05 \mu_B$ when the impurity concentration is 12.5%. The reason for this variation is not clear to us. For example, one could speculate that this could be a result of different hole concentrations in both spin-subbands. We should also mention a relatively large local moment on K-impurity which appears to be comparable to that induced on individual O-sites. It is few times larger than the local K-moment in ZrO_2 (0.10 and $0.08 \mu_B$).

The total and local DOSs for $\text{KTi}_7\text{O}_{16}$ supercell are shown in Fig. 3. The general trend is similar to that found for K-impurities in ZrO_2 : there is an impurity band in the minority DOS but less pronounced thus indicating a slightly weaker disorder due to K-impurities in TiO_2 as compared to ZrO_2 (see model calculations of Ref. [15]). The majority band is again only weakly perturbed and the system is metallic with the Fermi energy lying inside the valence band for both the majority and minority bands.

The spin resolved local DOS on O2 is weakly spin dependent for $\text{KTi}_7\text{O}_{16}$ supercell (see Fig. 3(c)). This results in a very small induced moment on these sites ($-0.05 \mu_B$). On the other hand, the O1 local DOS shows a halfmetallic behavior and gives rise to a larger induced moment ($0.28 \mu_B$). For lower concentration we observe a halfmetallic behavior for both O1 and O2 spin-resolved DOS (see Fig. 3(d)). This results in a similar size for the moment on O1 atoms but a significantly increased O2 moment (see Table 1).

3.3. Local magnetization around impurities in ZrO_2

The local magnetization $m(\mathbf{r})$ in [110]-plane around the impurity in real space is shown in Fig. 4 for $\text{KZr}_7\text{O}_{16}$ supercell. The small local moment on K is in the center of the plot with strongly damped Friedel-like oscillations. Such a damping is due to halfmetallic behavior of this system, i.e., the Fermi energy lies in the gap of the majority band. This feature is similar to that observed in the magnetic exchange couplings in the diluted magnetic semiconductors [23]. Large increase of the magnetization density in the neighborhood of the O-sites indicates the existence of an induced moment, few times larger than the local K-moment. The induced moments on the second shell of O-sites are also shown. Their magnitude is small but because the number of sites in the shell is relatively high (24), their contribution is non-negligible.

4. Conclusions

In conclusion, we have shown that a new path to controlled d^0 -ferromagnetism can be achieved by cation doping of oxides with carefully selected elements of the periodic table.

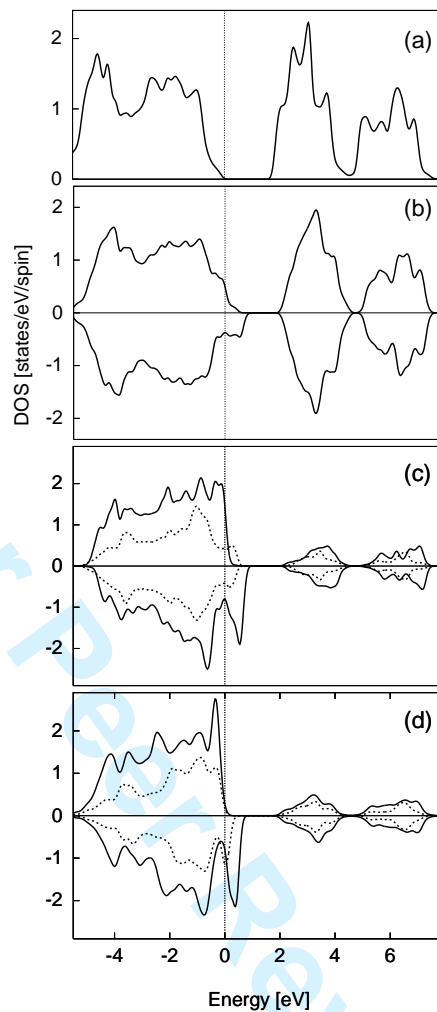


Figure 3. The total densities of states per formula unit for (a) TiO_2 host with the rutile structure and (b) spin resolved density of states for $\text{KTi}_7\text{O}_{16}$. The local spin-resolved densities of states on the first two O-shells (full and dotted lines) surrounding the impurity in the ferromagnetic cubic (c) $\text{KTi}_7\text{O}_{16}$ and (d) $\text{KTi}_{15}\text{O}_{36}$ that correspond to concentrations of 12.5% and 6.25%, respectively. The energy zero indicates the Fermi energy.

Specifically, we have shown that the promising systems are both cubic ZrO_2 and rutile TiO_2 materials doped with K (group 1A). The main conclusions of our study are: (i) The magnetic moment is mainly induced on the first oxygen shell neighboring the defect. (ii) A resonance peak near the top of the valence band in the minority channel is found, while the majority channel remains mainly unperturbed. This result is in agreement with a recent theoretical study based on model calculations [15]. (iii) The substitution by Ca (group 2A) has led to a non magnetic ground state. (iv) We have verified for a specific case that the total induced moment is robust with respect to lattice relaxations. (v) Our results also indicate that these effects are not inherent to a specific lattice structure.

The presence of an impurity band close to the top of the valence band is a precursor for the appearance of magnetism in dioxides. This is the case for both a vacancy and substitutional K-impurity. In contrast, for Ca substitution in cubic ZrO_2 , the impurity band is shifted deeper into the valence band, which prevents the formation of a magnetic moment.

An important question is whether these new materials could exhibit ferromagnetism above room temperature, i.e. whether the couplings are sufficiently large and extended? Our first results for cubic ZrO_2 [24] indicate a large ferromagnetic coupling ≈ 20 meV (240 K) and a simple estimate gives the Curie temperature above room temperature. The interesting and crucial issue which have to be addressed in the future are the impurity formation energies.

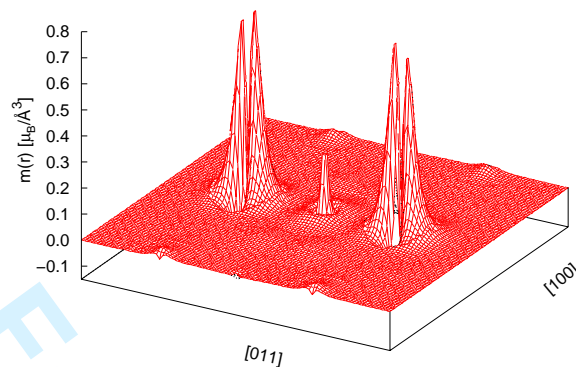


Figure 4. The local magnetization for the ferromagnetic cubic $\text{KZr}_7\text{O}_{16}$ supercell in the $[110]$ -plane. The K-impurity is in the center and two nearest neighbor O-atoms in the first O-shell, while four O-atoms in the second O-shell are visible at $[011]$ edges.

Acknowledgements

This work has been done within the project AVOZ1-010-0520 of the AS CR. We acknowledge the support from the Grant Agency of the Czech Republic, Contract No. 202/07/0456, COST P19-OC150 project and support from the Grant Agency of the Academy Sciences of the Czech Republic (A100100616).

References

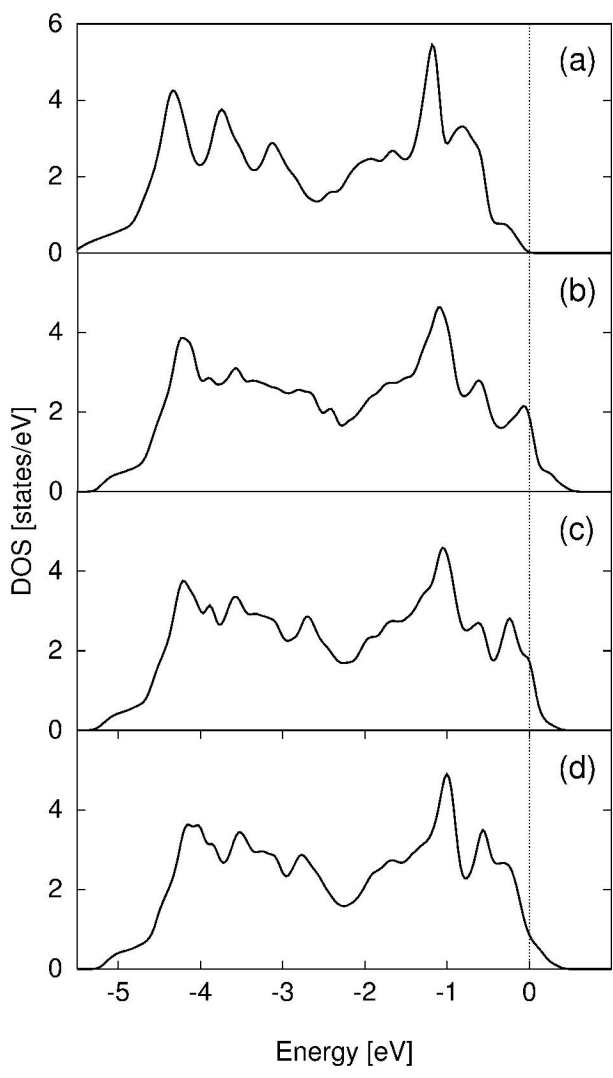
- [1] VENKATESAN, M., FITZGERALD, C.B., and COEY, J.M.D., 2004, *Nature (London)*, **430**, 630.
- [2] VENKATESAN, M., FITZGERALD, C.B., LUNNEY, J.G., and COEY, J.M.D., 2004, *Phys. Rev. Lett.*, **93**, 177206.
- [3] MAKAROVA, T.L., SUNDQVIST, B., HÖHNE, R., ESQUINAZI, P., KOPELEVICH, Y., SCHARFF, P., DAVYDOV, V., KASHEVAROVA, L.S., and RAKHMANINA, A.V., 2001, *Nature (London)*, **413**, 716.
- [4] ESQUINAZI, P., SETZER, A., HÖHNE, R., SEMMELHACK, C., KOPELEVICH, Y., SPEMANN, D., BUTZ, T., KOHLSTRUNK, B., and LÖSCHE, 2002, *Phys. Rev. B*, **66**, 024429.
- [5] YOUNG, D.P., FISK, Z., THOMPSON, J.D., OTT, H.R., OSEROFF, S.B., and GOODRICH, R.G., 1999, *Nature (London)*, **397**, 412.
- [6] TASAKI, H., 1995, *Phys. Rev. Lett.*, **75**, 4678.
- [7] MIELKE A., 1999, *Phys. Rev. Lett.*, **82**, 4312.
- [8] SIEBERER, M., REDINGER, J., KHMELEVSKIY, S., and P. MOHN, P., 2006, *Phys. Rev. B*, **73**, 024404.
- [9] MATSUBAYASHI, K., MAKI, M., TSUZUKI, T., NISHIOKA, T., and SATO, N., *Nature (London)*, **420**, 143.
- [10] STONEHAM, A.M., PATHAK, A.P., and BARTRAM, R.H., 1976, *J. Phys. C: Solid State Phys.*, **9**, 73.
- [11] ELFIMOV, I.S., YUNOKI, S., and SAWATZKY, G.A., 2002, *Phys. Rev. Lett.*, **89**, 216403.
- [12] DAS PEMMARAJU, C., and SANVITO, S., *Phys. Rev. Lett.*, 2005, **94**, 217205.
- [13] OSORIO-GUILLEN, J., LANY, S., BARABASH, S.V., and ZUNGER, A., 2006, *Phys. Rev. Lett.*, **96**, 107203.
- [14] COEY, J.M.D., VENKATESAN, M., STAMENOV, P., FITZGERALD, C.B., and DORNELES, L.S., 2005, *Phys. Rev. B*, **72**, 024450.
- [15] BOUZERAR, G. and ZIMAN, T., 2006, *Phys. Rev. Lett.*, **96**, 207602.
- [16] BLAHA, P., SCHWARZ, K., MADSEN, G.K.H., KVASNICKA, D., and LUITZ, J., 2001, *WIEN2k, An Augmented Plane Wave + Local Orbitals Program for Calculating Crystal Properties* (Wien, Austria: Karlheinz Schwarz, Techn. Universität), ISBN 3-9501031-1-2.
- [17] BAYER, G., 1970, *J. Am. Ceram. Soc.*, **53**, 294.
- [18] STRAUMANIS, M.E., EJIMA, T., and JAMES, W.J., 1961, *Acta Cryst.*, **14**, 493.
- [19] PERDEW, J. P., and WANG, Y., 1992, *Phys. Rev. B*, **45**, 13244.
- [20] LAZAROVITS, B., SZUNYOGH, L., and Weinberger, P., 2002, *Phys. Rev. B*, **65**, 104441.
- [21] TUREK, I., DRCHAL, V., KUDRNOVSKÝ, J., ŠOB, M., and WEINBERGER, P., 1997, *Electronic Structure of Disordered Alloys, Surfaces and Interfaces* (Boston, Massachusetts: Kluwer).
- [22] Turek, I., Kudrnovský, J., and DRCHAL, V., 2000, in *Electronic Structure and Physical Properties of Solids*, edited by DREYSSÉ, H., Lecture Notes in Physics, Vol. **535** (Berlin: Springer), p. 349.
- [23] KUDRNOVSKÝ, J., TUREK, I., DRCHAL, V., MÁČA, F., WEINBERGER, P., and BRUNO, P., 2004, *Phys. Rev. B*, **69**, 115208.

[24] MÁCA, F., KUDRNOVSKÝ, J., DRCHAL, V., and BOUZERAR, G., 2008, *Appl. Phys. Lett.*, in print.

For Peer Review Only

1
2
3
4
5
6
7
8
9
10
11
12
13
14
15
16
17
18
19
20
21
22
23
24
25
26
27
28
29
30
31
32
33
34
35
36
37
38
39
40
41
42
43
44
45
46
47
48
49
50
51
52
53
54
55
56
57
58
59
60

1
2
3
4
5
6
7
8
9
10
11
12
13
14
15
16
17
18
19
20
21
22
23
24
25
26
27
28
29
30
31
32
33
34
35
36
37
38
39
40
41
42
43
44
45
46
47
48
49
50
51
52
53
54
55
56
57
58
59
60



177x319mm (600 x 600 DPI)

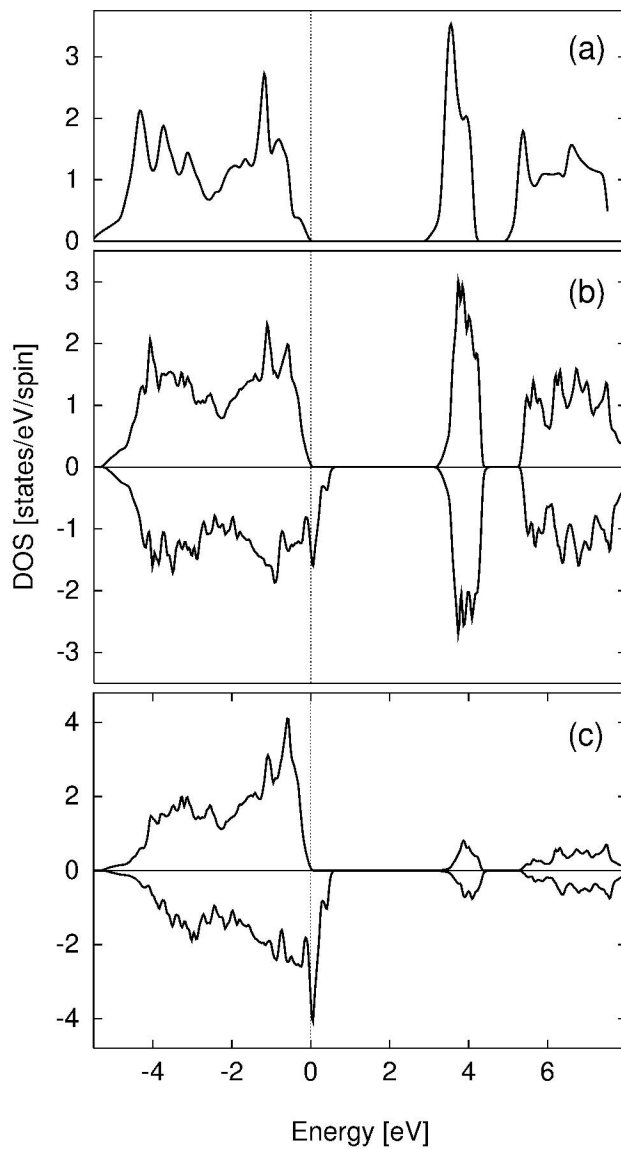


Figure 2
177x317mm (600 x 600 DPI)

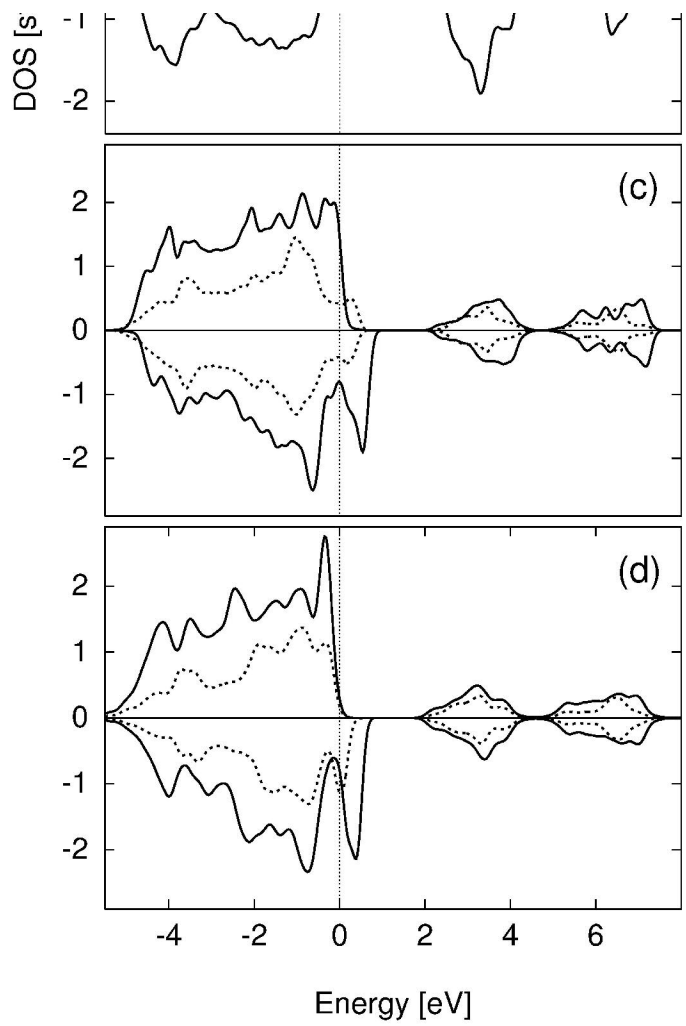


Figure 3
215x279mm (600 x 600 DPI)

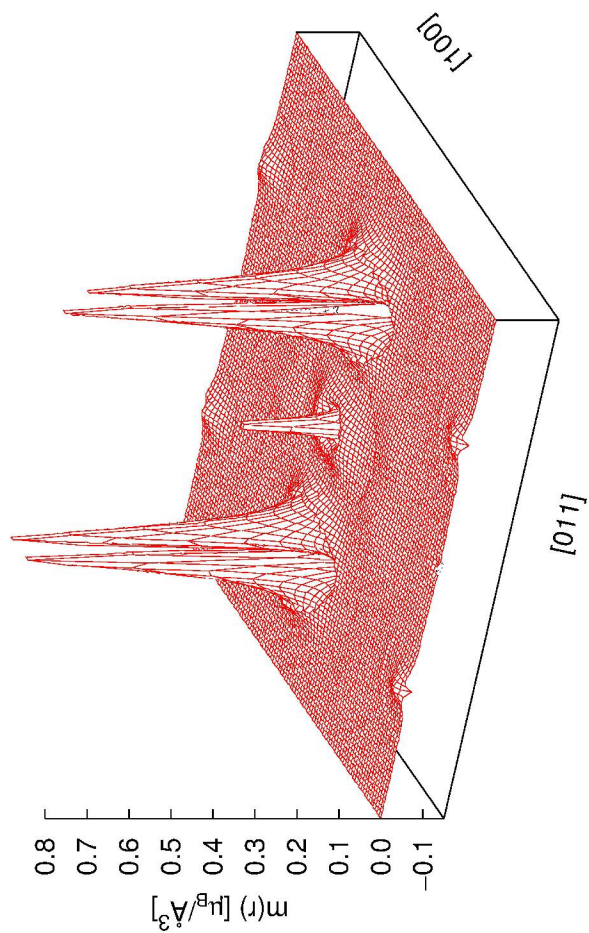


Figure 4
215x279mm (600 x 600 DPI)

1
2
3
4
5
6
7
8
9
10
11
12
13
14
15
16
17
18
19
20
21
22
23
24
25
26
27
28
29
30
31
32
33
34
35
36
37
38
39
40
41
42
43
44
45
46
47
48
49
50
51
52
53
54
55
56
57
58
59
60